Title

Interaction of p55 Reverse Transcriptase from theSaccharomyces cerevisiae Retrotransposon Ty3 with Conformationally Distinct Nucleic Acid Duplexes*

Journal

Journal of Biological Chemistry, 275(18)

ISSN

0021-9258

Authors

Rausch, Jason W
Grice, Marion K Bona-Le
Henrietta, M
et al.

Publication Date

2000-05-01

DOI

10.1074/jbc.275.18.13879

THE JOURNAL OF BIOLOGICAL CHEMISTRY Vol. 275, No. 18, Issue of May 5, pp. 13879–13887, 2000
Printed in U.S.A.

Interaction of p55 Reverse Transcriptase from the *Saccharomyces cerevisiae* Retrotransposon Ty3 with Conformationally Distinct Nucleic Acid Duplexes*

Received for publication, January 21, 2000

Jason W. Rausch‡§, Marion K. Bona-Le Grice§¶, M. Henrietta, Nymark-McMahon‖, Jennifer T. Miller‡, and Stuart F. J. Le Grice‡

From the ‡Human Immunodeficiency Virus Drug Resistance Program, Division of Basic Sciences, NCI-Frederick Cancer Research and Development Center, Frederick, Maryland 21702, ¶Science Applications International Corporation, Frederick, Maryland 21702, and the ‖Department of Biological Chemistry, College of Medicine, University of California, Irvine, California 92697-1700

The 55-kDa reverse transcriptase (RT) domain of the Ty3 *POL3* open reading frame was purified and evaluated on conformationally distinct nucleic acid duplexes. Purified enzyme migrated as a monomer by size exclusion chromatography. Enzymatic footprinting indicate Ty3 RT protects template nucleotides +7 through −21 and primer nucleotides −1 through −24. Contrary to previous data with retroviral enzymes, a 4-base pair region of the template-primer duplex remained nuclease accessible. The C-terminal portion of Ty3 RT encodes a functional RNase H domain, although the hydrolysis profile suggests an increased spatial separation between the catalytic centers. Despite conservation of catalytically important residues in the RNase H domain, Fe^{2+} fails to replace Mg^{2+} in the RNase H catalytic center for localized generation of hydroxyl radicals, again suggesting this domain may be structurally distinct from its retroviral counterparts. RNase H specificity was investigated using a model system challenging the enzyme to select the polypurine tract primer from within an RNA/DNA hybrid, extend this into (+) DNA, and excise the primer from nascent DNA. Purified RT catalyzed each of these three steps but was almost inactive on a non-polypurine tract RNA primer. Our studies provide the first detailed characterization of the enzymatic activities of a retrotransposon reverse transcriptase.

Following infection, retroviruses initiate their DNA synthesis program from a host-derived tRNA hybridized to a specific region at the 5′ end of their (+) strand RNA genome, designated the primer binding site or PBS.[1] However, tRNA use is somewhat heterogeneous, *i.e.* while avian viruses exploit $tRNA^{Trp}$, Moloney murine leukemia virus uses $tRNA^{Pro}$ and D-type and human spumaretroviruses $tRNA^{Lys1,2}$ (1). In the case of HIV and related lentiviruses of simian, feline, and equine origin, $tRNA^{Lys3}$ is selected as the replication primer. Early experimentation suggested complementarity between the PBS and sequences at the 3′ terminus of the replication primer as the sole specificity determinant during initiation of (−) strand synthesis (2). However, extensive analyses with Rous sarcoma virus (3–5) and HIV-1 (6–14) have provided a convincing argument that additional intermolecular base pairing between the replication primer and sequences of the viral genome 5′ to the PBS play a major role in controlling initiation. In the latter case, chemical footprinting data (11, 15) and kinetic analysis (12, 14) indicate a two-step initiation program. The first of these is characterized by slow addition of the first 5 dNTPs, during which DNA synthesis is highly distributive; subsequently, the replication machinery moves into a rapid and processive elongation mode. Avian viruses display a similar control mechanism, although the intermolecular interactions underlying this are subtly different, *i.e.* while the anticodon loop of $tRNA^{Lys,3}$ is in intimate contact with U5-IR loop bases of the HIV genome, this occurs between the TΨC arm of $tRNA^{Trp}$ and U5-IR stem bases in Rous sarcoma virus (3–5).

Although restricted to an intracellular life cycle in the absence of an envelope gene, LTR-containing retrotransposons of the budding yeast *Saccharomyces cerevisiae,* representatives of which include Ty1 and Ty3, share many features of the reverse transcription cycle with their retroviral counterparts (16). Both are LTR-containing elements requiring a host-derived tRNA primer, in this case $tRNA_i^{Met}$, to initiate (−) strand synthesis. In contrast, a distinguishing feature of these retrotransposons is the limited complementarity between PBS sequences at the 5′ end of the genome and the tRNA primer, which in Ty3 is reduced from 18 to 8 nt. However, Keeney *et al.* (17) demonstrated that features of the TΨC arm are critical to transposition, and more recently Gabus *et al.* (18) provided experimental evidence that Ty3 compensates for this by exploiting a bipartite PBS. According to this model, a region with extensive complementarity (12 nucleotides) to the TΨC arm of the tRNA primer is located at the 3′ end of the genome. Although speculative, these authors have also suggested an initiation complex of two genomic RNAs could be stabilized through a short autocomplementary sequence in $tRNA_i^{Met}$, which induces dimerization. A similar scenario prevails with Ty1, where reduced complementarity to the 3′ end of the tRNA primer (10 nt) is compensated by extended interactions with the D arm (19). This notion of co-operativity between distal *cis*-acting sequences on the genome may be not be unique to retrotransposons. Brule *et al.*

* This work was supported in part by National Institutes of Health Grants GM 52263 (to S. F. J. L. G.) and GM33281 (H. M. N.-M.). The costs of publication of this article were defrayed in part by the payment of page charges. This article must therefore be hereby marked "*advertisement*" in accordance with 18 U.S.C. Section 1734 solely to indicate this fact.

§ These authors contributed equally to this work.

** To whom correspondence should be addressed: HIV Drug Resistance Program, Div. of Basic Sciences, NCI-FCRDC, Bldg. 535, Frederick, MD 21702. Tel.: 301-846-5256; Fax: 301-846-6013; E-mail: slegrice@mail.ncifcrf.gov.

[1] The abbreviations used are: PBS, phosphate-buffered saline; FIV, feline immunodeficiency virus; RT, reverse transcriptase; HIV, human immunodeficiency virus; IPTG, isopropyl-1-thio-β-D-galactopyranoside; PPT, polypurine tract; LTR, long terminal repeat; nt, nucleotide(s); bp, base pair(s); IN, integrase; EIAV, equine infectious anemia virus; MLV, Moloney murine leukemia virus.

(20) have found that (−) strand transfer in HIV can benefit from complementary sequences in the tRNA anticodon stem and bases in the U3 region at the 3′ end of the genome. A better understanding of *cis*-acting sequences cooperating in (−) strand DNA synthesis in retrotransposons would therefore be beneficial.

As in retroviruses, (+) strand synthesis in retrotransposons initiates from an RNase H-resistant, purine-rich sequence immediately adjacent to the U3 region at the 3′ end of the genome and designated the polypurine tract or PPT. This sequence must be (i) selected from the (+) RNA/(−) DNA replication intermediate, (ii) extended at its 3′ terminus into (+) strand DNA, and (iii) excised from the nascent (+) strand to generate the appropriate 5′ LTR sequences for recognition by the integration machinery. Since imprecise removal of the PPT from (+) DNA may have consequences for integration, PPT selection and removal must by necessity be a highly accurate process. In this respect, Kirchner and Sandmeyer (21) and Wilhelm *et al*. (22) indicated that several ribonucleotides at the 3′ terminus of the Ty3 and Ty1 PPT could serve as (+) strand initiation sites. These studies have relied exclusively on analysis of DNA isolated from virus-like particles since, until recently, purified Ty3 RT and a reconstituted system recapitulating *in vivo* events have been unavailable. The goal of the present study was to prepare recombinant Ty3 RT and analyze both the nucleoprotein complexes and enzymatic activities (DNA polymerase and RNase H) mediating these events. DNase I footprinting of binary polymerization complexes indicates an organization unlike that demonstrated for several retroviral enzymes (23–25). A system of "PPT scanning" was also exploited to evaluate the precision with which Ty3 (+) strand synthesis is initiated. Surprisingly, this system indicated that the specificity of primer selection and removal was dependent on the nature of the PPT-containing RNA primer. Finally, alignment of amino acid sequences from the RNase H domains of several LTR-containing retrotransposons and plant caulimoviruses suggests an alternative distribution of catalytic residues.

EXPERIMENTAL PROCEDURES

Cloning, Expression, and Purification of Ty3 RT

The 55-kDa RT open reading frame was amplified from the Ty3 *POL3* gene (26) by the polymerase chain reaction as a *Bam*HI/*Hin*dIII fragment and inserted between the equivalent sites of plasmid p6HRT (27). This procedure generated plasmid p6HTy3RT, which allows IPTG-inducible expression of a polyhistidine extended enzyme. RT was purified from logarithmically grown and IPTG-induced cultures by a combination of metal chelate (nickel-nitrilotriacetic acid-Sepharose) and ion exchange chromatography (S-Sepharose). Purified enzyme was demonstrated to be free of contaminating nucleases and stored at −20 °C in a 50% glycerol-containing buffer (28) at a concentration of 0.25 mg/ml. Under these conditions, we observed minimal loss of DNA polymerase or RNase H activity over several months.

For comparative purposes, the p66/p51 form of either FIV or HIV-1 RT was included in several experiments. Methods for preparation and purification of these enzymes have been provided elsewhere (28). Immunological analysis of Ty3 RT expressed in *Escherichia coli* was performed using rabbit polyclonal antibodies against the purified protein.

Determination of Ty3 RT Subunit Composition

The molecular weight and quaternary structure of Ty3 RT was evaluated by size exclusion chromatography using a Superdex 200 HR 10/30 column (Amersham Pharmacia Biotech) connected to a DuoFlow (Bio-Rad) chromatography system. For Calibration purposes, 50–250 μg of several proteins of known molecular weight were applied to the column in a buffer of 50 mM Tris HCl (pH 7.0), 25 mM NaCl, 1 mM EDTA at a flow rate of 0.4 ml/min. These include human IgG (150,000 Da), HIV RT p66/p51 (117,000 Da), bovine serum albumin (67,000 Da), HIV RT p51 (52,000 Da), β-lactoglobulin (35,000 Da), and cytochrome *c* (12,000 Da). 62 μg of Ty3 RT was likewise applied. Elution of proteins was detected spectrophotemetrically (E_{280}), and migration times plotted against log molecular weight to create a molecular weight standard curve. The best fit dependence of mass on migration time was determined using the logarithmic curve-fitting function of Delta Graph graphing software (Design Sciences, Inc.).

DNA Polymerase Activity

DNA-dependent DNA polymerase activity was evaluated on a 71-nt template hybridized to a 5′ end-labeled 36-nt primer, the former of which contains a short stem-loop in the single stranded template (29). Twenty nM template-primer (annealed by incubation at 95 °C in 10 mM Tris/HCl, pH 7.5, 25 mM $MgCl_2$ and slow cooling to room temperature) was incubated with 40 nM RT on ice for 5 min, in a buffer comprising 10 mM Tris/HCl, pH 7.5, 10 mM $MgCl_2$, 50 mM KCl, and 5 mM dithiothreitol. DNA synthesis was initiated at 30 °C by addition of dATP, dGTP, dCTP, and TTP to a final concentration of 100 μM. Aliquots were removed at times indicated in the text and mixed with an equal volume of 7 M urea containing 0.1% bromphenol blue and xylene cyanol. Polymerization products were resolved by high voltage denaturing polyacrylamide gel electrophoresis and evaluated by autoradiography.

RNase H Activity

RNase H activity was initially evaluated on a 5′ end-labeled 90-nt RNA template (prepared by *in vitro* transcription) hybridized to the 36-nt DNA primer used to evaluate polymerase function (30). 10 nM enzyme was incubated with 20 nM template-primer in a buffer containing 10 mM Tris/HCl, pH 7.5, 50 mM KCl, 5 mM dithiothreitol. Hydrolysis was initiated by addition of $MgCl_2$ to a final concentration of 10 mM and allowed to continue at 30 °C. Aliquots were again removed at times indicated in the text and processed as described above. In a minor modification to this technique, RNase H activity was also examined on the same substrate whose 3′ terminus was end-labeled with [^{32}P]Cp and RNA ligase (New England Biolabs) under conditions recommended by the manufacturer.

Enzymatic Footprinting of Replication Complexes

DNase I—DNase I footprinting (24) was conducted on the 71-nt template/36-nt primer described above and whose template or primer was end-labeled with γ-^{32}P and polynucleotide kinase. End-labeling followed protocols specified by the manufacturer (Roche Molecular Biochemicals). 50 mM end-labeled template-primer was incubated with 85 nM Ty3 RT in 10 mM Tris/HCl, pH 8.0, 6 mM $MgCl_2$, 80 mM NaCl for 10 min at room temperature. Two units of DNase I were added, and digestion allowed to proceed for 30 s. Hydrolysis was terminated by addition of an equal volume of phenol/chloroform/isoamyl alcohol (25:24:1). Nucleic acids in the aqueous phase were recovered by ethanol precipitation; dried; resuspended in a solution of 8 M urea, 0.1% bromphenol blue, and 0.1% xylene cyanol; and fractionated by high voltage denaturing polyacrylamide gel electrophoresis. Hydrolysis products were visualized by autoradiography.

S1 Nuclease—S1 footprinting (24) required modification of the DNase I protection protocol. Following preparation of protein/nucleic acid complexes, the sample was supplemented with 40 units of S1 (Roche Molecular Biochemicals) in a concentrated S1 buffer, such that the final composition of the reaction mixture was 33 mM sodium acetate, pH 4.5, 50 mM NaCl, and 30 μM $ZnSO_4$. Following 30 s of S1 treatment, hydrolysis was terminated and nucleic acids processed as described above. Under these conditions, the replication complex remains stable over the digestion period. Control S1 digests of extended substrates in the absence of RT were also prepared.

Polypurine Tract Utilization

Experiments evaluating Ty3 PPT utilization required a combination of both DNA polymerase and RNase H activities (31). A 65-nt, chemically synthesized (−) strand DNA template (Integrated DNA Technologies) containing the PPT complement was hybridized to synthetic (+) strand RNA primers (Dharmacon Research) spanning the PPT by heating to 90 °C and slow cooling in 10 mM Tris/HCl, pH 7.5, 25 mM $MgCl_2$. The final concentration of all template-primer combinations following hybridization was 20 μM.

These substrates were incubated at room temperature for 45 min with Ty3 RT in buffer containing (final concentration) 10 mM Tris/HCl, pH 8.0; 80 mM NaCl; 6 mM $MgCl_2$; 5 mM dithiothreitol; 1 μM template-primer; 340 nM RT; 100 μM each dATP, dGTP, dCTP, and TTP; 85 nM [α-^{32}P]dATP. After 45 min, the reactions were terminated by heating to 90 °C for 2 min, after which unincorporated radioactivity was removed by spin-column Sephadex G25 gel filtration (Amersham Pharmacia Biotech). The eluate was divided into equal portions to visualize nascent (+) DNA containing or lacking the RNA primer. One portion was

treated with 0.3 volumes of 1 N NaOH at 65 °C to hydrolyze all RNA primers, then neutralized by adding an equivalent volume of 1 N HCl. Nucleic acids were precipitated with ethanol; precipitated; dried; and resuspended in 7 M urea, 0.1% bromphenol blue, and 0.1% xylene cyanol. The remaining portion (*i.e.* containing RNA primers) was precipitated as described above and resuspended in the same gel loading buffer. DNA synthesis products were fractionated by high voltage denaturing polyacrylamide gel electrophoresis and visualized by autoradiography.

Fe^{2+}-mediated Cleavage of Duplex DNA by the RNase H Domain

Replacement of Mg^{2+} in the RNase H domain with Fe^{2+} and hydroxyl radical-mediated cleavage of duplex DNA followed the protocol of Goette *et al.* (32). Substrate was the 71-nt template/36-nt primer used to evaluate DNA-dependent DNA polymerase activity, the template of which was 5′ end-labeled with [γ-^{32}P]ATP and polynucleotide kinase according to standard protocols. Enzyme (1 μM) and template primer (50 nM) were incubated 5 min at room temperature in a buffer of 80 mM HEPES, pH 8.0, 50 mM NaCl. The following reactants were subsequently pipetted onto the wall of the reaction tube: 1 μl of 50 mM dithiothreitol, 1 μl of freshly prepared H_2O_2, 2 μl of 2 mM $Fe(NH_4)2(SO_4)_2{\cdot}6H_2O$. Reaction vessels were carefully closed and centrifuged to initiate of Fe^{2+}-mediated hydroxyl radical cleavage. After 5 min, the reaction was terminated by adding 40 μl of stop solution (0.1 M thiourea, 10.0 mM EDTA, 0.6 M NaOAc, pH 6.2), and 1 μl of glycogen. Nucleic acids were precipitated with ethanol, collected by centrifugation, dried, and resuspended in urea-based gel loading buffer. Hydrolysis products were fractionated by high voltage denaturing gel electrophoresis and visualized by autoradiography.

RESULTS

Purified p55 Ty3 RT Sediments as a Monomer—Although most lentiviral RTs studied to date exhibit a dimeric structure of asymmetrically organized subunits, the purified MLV enzyme is a monomer. Although surprising, the possibility of a monomeric RT organization is supported by recent data with recombinant enzyme from bovine leukemia virus (33), which was shown by rate sedimentation analysis to migrate as a monomer in both the absence and presence of duplex DNA. Following expression and purification of Ty3 RT (Fig. 1, *A* and *B*), its quaternary structure was evaluated by size exclusion chromatography. As indicated in Fig. 1*B*, the Ty3 enzyme migrated slightly faster than the monomeric polyhistidine-tagged p51 subunit of HIV-1 RT (mass 52 kDa) but behind bovine serum albumin (mass 67 kDa), which is consistent with a monomeric organization. However, these results do not rule out the possibility of other RT forms are required during Ty3 replication.

DNA-dependent DNA Polymerase Activity of Ty3 RT—The ability of Ty3 RT to support processive DNA synthesis in the absence of accessory factors such as the nucleocapsid protein was initially assessed. At the same time, we also wished to determine the extent to which processivity might be influenced by temperature, since yeast strains harboring Ty elements are maintained at 30 °C and RT activity in VLPs is temperature-sensitive (34). DNA synthesis was evaluated on a 71-nt DNA template/36-nt DNA primer used to characterize many of the retroviral RTs in our collection (24). A fortuitous feature of this substrate is the intramolecular duplex adopted by the single-stranded template immediately ahead of the primer 3′ terminus (Fig. 2*A*). This structure has been exploited to evaluate the processivity of wild type and mutant variants of HIV-1 and EIAV RT. As an example, Wöhrl *et al.* demonstrated that the p51 subunit of EIAV RT efficiently initiates DNA synthesis on this substrate, but fails to polymerize into the hairpin (29). A similar phenotype was obtained with HIV-1 enzymes harboring mutations within the p66 primer grip motif (35). Thus, as a preliminary characterization, the response of the Ty3 enzyme to this structure was investigated, the results of which are presented in Fig. 2 (B and C).

DNA polymerase activity of Ty3 RT was affected by both the

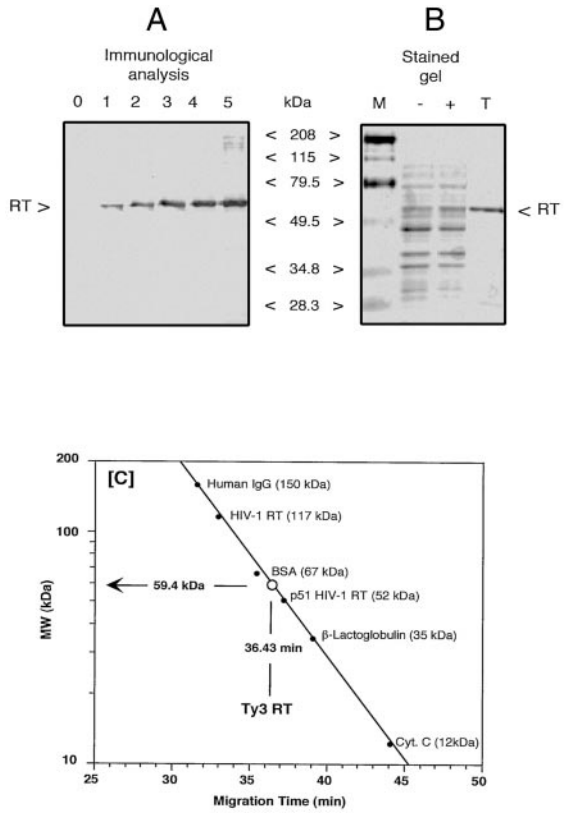

FIG. 1. *A*, immunological evaluation of Ty3 RT expression in recombinant *E. coli*. M15:pDM1.I::p6HTy3RT was grown to mid-log phase and induced with IPTG as outlined under "Experimental Procedures." Samples were withdrawn after for 15, 30, 45, 60, and 120 min (*lanes 1–5*, respectively) and analyzed with antiserum against Ty3 RT. *Lane 0*, pre-IPTG induction sample. *B*, evaluation of Ty3 RT expression and purification by Coomassie Blue staining. *Lane −*, pre-IPTG induction; *lane +*, 45 min post-IPTG induction; *lane T*, purified Ty3 RT; *lane M*, molecular weight markers. *C*, determination of Ty3 RT subunit stoichiometry by size exclusion chromatography. Molecular weights of standard proteins have been indicated on the calibration curve.

template hairpin and temperature at which the assay was performed (Fig. 2*B*). At 37 °C, *i.e.* where the HIV-1 enzyme was most active, DNA-dependent DNA synthesis catalyzed by Ty3 RT stopped predominantly between positions P + 10 and P + 15, which define the base of the template hairpin (Fig. 2*A*). Since DNase I and S1 footprinting experiments have verified the presence of the stem-loop (24), it appears that Ty3 RT inefficiently resolves this structure at 37 °C. Lowering the incubation temperature to 30 °C conferred on Ty3 RT the capacity to polymerize through the hairpin, although the overall level of polymerase activity was lower than that obtained with the HIV-1 enzyme. In Fig. 2*C*, a time course of DNA-dependent DNA synthesis was performed with both the HIV-1 and Ty3 enzymes at 30 °C. Although it is again clear that Ty3 RT is less active than its HIV-1 counterpart, pausing between template nucleotides +10 and +15 is only observed with the latter, suggesting the Ty3 enzyme may have a more robust strand displacement activity.

Enzymatic Footprinting of Ty3 Replication Complexes—Enzymatic footprinting of HIV (24), EIAV (25), and MLV replication complexes (23) indicates that the retroviral polymerase is in close contact with DNA from template nucleotide +7 to −24/−27 of the template-primer duplex. Since the size of the Ty3 enzyme is considerably different from those we have previously evaluated, it was of interest to determine if this resulted in an altered enzymatic footprint on the same template-primer duplex. A complete picture of the nucleoprotein complex

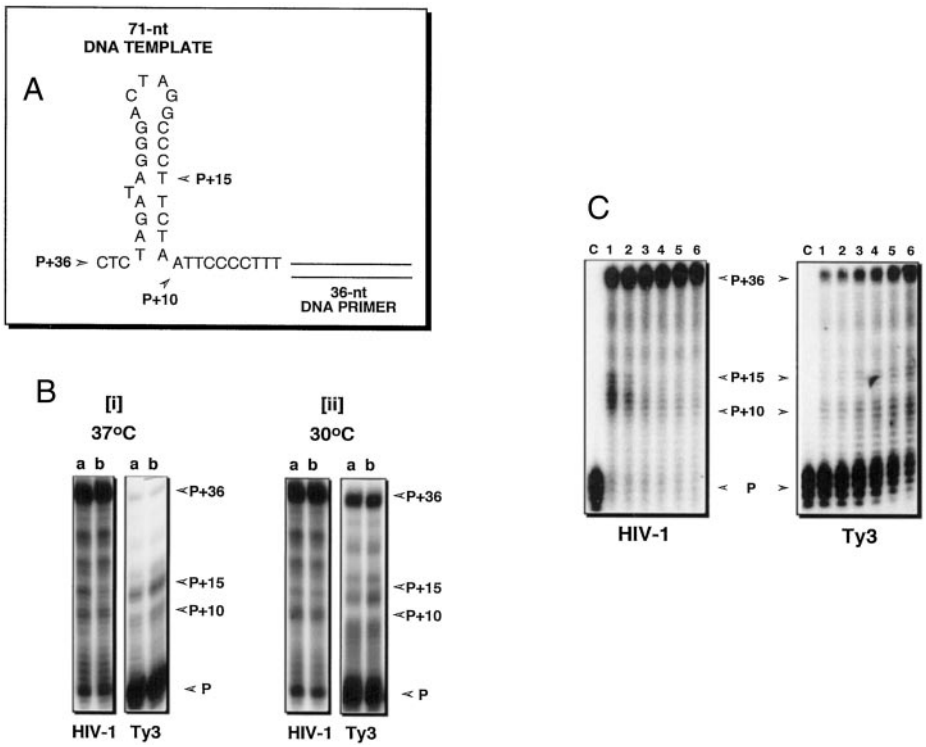

FIG. 2. **DNA-dependent DNA polymerase activity of purified Ty3 reverse transcriptase.** *A*, schematic representation of the heteropolymeric substrate, comprising a 71-nt template to which a 5′ labeled 36-nt primer is hybridized. Note that a region near the 5′ end of the single-stranded template has the capacity for intramolecular base pairing. Stalling of RT in this region is characterized by accumulation of P + 10 to P + 15 products. *B*, temperature sensitivity of DNA polymerase activity catalyzed by HIV-1 and Ty3 RT. For each temperature indicated, duplicate 10 min DNA synthesis profiles (*a* and *b*) are presented. *C*, time course of Ty3 and HIV-1 RT-catalyzed DNA synthesis at 30 °C. *Lanes C*, radiolabeled primer (36 nt). In both cases, DNA synthesis was evaluated after 1 min (*lanes 1*), 2 min (*lanes 2*), 5 min (*lanes 3*), 10 min (*lanes 4*), 20 min (*lanes 5*), and 45 min (*lanes 6*). Note that, whileTy3 RT is less active than the HIV-1 enzyme, stalled products in the range P + 10 to P + 15 are absent.

can only be achieved by independent evaluation of resistance to the nucleases S1 and DNase I, which hydrolyze single-stranded and double-stranded DNA, respectively (Fig. 3*A*). For comparison, replication complexes containing p66/p51 HIV-1 RT were evaluated in parallel.

The results of S1 probing are illustrated in Fig. 3*B*. Since the single-stranded template of our substrate assumes an intramolecular base paired structure (Fig. 3*A*), only template nucleotides between positions +1 and +10 are revealed in Fig. 3*B* (hydrolysis products in the immediate vicinity of the 5′ terminus lie outside the resolving capacity on the gel). Incubation of template-primer with the heterodimeric HIV-1 enzyme results in protection of template nucleotides between positions +1 and +7 from hydrolysis, which is in keeping with our previous findings (23, 24). A similar S1 hydrolysis profile was obtained with the Ty3 enzyme, suggesting that the finger subdomains of each polymerase make equivalent contact with nucleotides ahead of the DNA polymerase catalytic center. In contrast, the manner in which the HIV-1 and Ty3 enzymes contact the template-primer duplex is significantly different (Fig. 3*C*). The protection pattern derived from the HIV-1 enzyme extends as far as template nucleotide −22, within which positions −19/−20 remain nuclease-accessible. In the presence of Ty3 RT, the protection pattern extends to position −24, while template nucleotides between positions −16 and −19 remain nuclease-accessible. A similar pattern emerges when contact to primer nucleotides of the template-primer duplex is investigated (Fig. 3*D*). In this case, HIV-1 RT protects primer nucleotides between positions −1 and −25, within which positions −19/−20 remain accessible. With the Ty3 enzyme, the protection pattern also extends as far as primer nucleotide −25, but within this footprint positions −16 to −18 are rendered nuclease-susceptible. Combining the Ty3 RT-derived template and primer hydrolysis profiles suggests duplex DNA between positions −16 and −19 remains freely accessible to DNase I. Such data may indicate that the N-terminal DNA polymerase and C-terminal RNase H domains of Ty3 RT form independent domains separated by a small linker, as has been proposed for the murine enzyme (36). Alternatively, an interaction of Ty3 RT with the template-primer duplex may alter its structure sufficiently to render it locally hypersensitive to DNase I digestion.

RNase H Hydrolysis Profiles Suggest an Altered Spatial Separation between the DNA Polymerase and RNase H Domains of TY3 RT—Currently available crystallographic (37–39), enzymatic (31, 40), and chemical probing data (41) suggest that the DNA polymerase and RNase H domains of the retroviral polymerase are separated by 17–18 bp. In order to determine whether the same holds for the Ty3 enzyme, its interaction with an RNA/DNA hybrid related to the DNA duplex of the previous section was evaluated. This substrate is depicted in Fig. 4*A*, comprising a 90-nt RNA template to which the identical 36-nt DNA primer is hybridized. The temporal sequence of RNase H-mediated hydrolysis is indicated in Fig. 4A and involves initial endonucleolytic cleavage at position −17, followed by a directional processing activity extending to position −8. Using the system illustrated in Fig. 4A, these activities are diagnosed by the accumulation of 71- and 62-nt hydrolysis fragments, respectively.

RNase H-mediated hydrolysis catalyzed by HIV-1 RT is illustrated in Fig. 4*B*. Initially, hydrolysis products of 71, 74, and, to a lesser extent, 76 nt accumulate, and are gradually replaced by fragments in the range 64–62 nt. A similar pattern emerges when Ty3 RNase H-mediated hydrolysis is evaluated, but differs significantly in the size of the hydrolysis products.

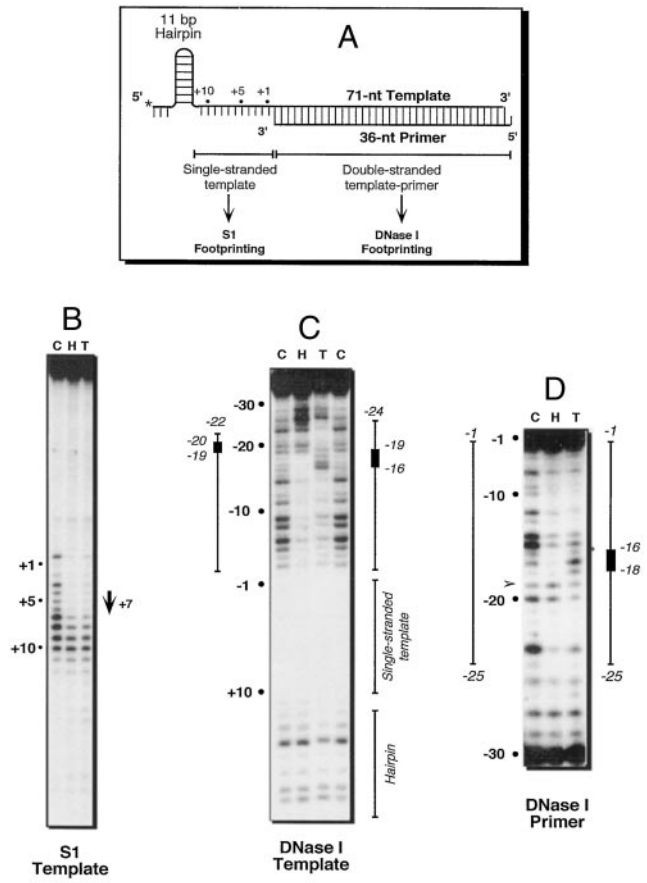

FIG. 3. **Enzymatic footprinting of Ty3 RT.** The substrate depicted in *panel A* is that used to evaluate DNA-dependent DNA polymerase activity. The presence of an 11-bp stem-loop near the 5′ terminus of the template generates a substrate that is resistant to nuclease S1 and sensitive to DNase I. *Panel B*, S1 footprinting of contacts made to the single-stranded template ahead to the DNA polymerase catalytic center. *C*, no enzyme; *H*, p66/p51 HIV-1 RT; *T*, Ty3 RT. As indicated above, intramolecular template base pairing has the consequence that only template bases between positions +1 and +10 are revealed. *Panel C*, interaction of HIV-1 (*lane H*) and Ty3 RTs (*lane T*) with the template strand of the template-primer duplex. *Lanes C*, no enzyme. Template nucleotides within each footprint that retain DNase I sensitivity or display hyper-reactivity have been boxed. The positions of the single-stranded template and intramolecular hairpin have been indicated at the *side* of the panel. *Panel D*, interaction of HIV-1 and Ty3 RTs with primer nucleotides of the template-primer duplex. Template nucleotides that are hyper-reactive in the presence of the HIV-1 and Ty3 enzyme have been indicated by the *arrow* and *closed box*, respectively. Lane designations are as in *panel C*.

Accumulation of a 75-nt fragment at early stages represents hydrolysis at template nucleotide −21. Subsequent to this, the final product of directional processing is a 65-nt fragment, indicating cleavage at template nucleotide −11. While we have previously provided evidence that different lentiviral RTs may have a more stringent separation between their catalytic centers (37–39), Ty3 is the first RT shown to terminate directional processing at this position. In the experiment of Fig. 3*C*, hydrolysis was evaluated on the same substrate but whose RNA template was labeled at the 3′ terminus. Since RT binding is initially controlled by the DNA primer 3′ terminus, the combination of synthesis-dependent and -independent RNase H activities will have the effect of producing a "gapped" template. In doing so, this directs re-binding of RT for cleavage further downstream, *i.e.* toward the radiolabel, thereby generating short hydrolysis products (31). This bimodal hydrolysis is evident for both the HIV-1 and Ty3 enzymes, but, as was demonstrated with the 5′ labeled substrate, the distribution of hydrolysis products is significantly different.

Ty3 RT Fails to Support Fe-mediated Cleavage of Duplex DNA—Goette *et al.* (32, 42) have elegantly demonstrated that Fe^{2+} can be substituted for Mg^{2+} in the RNase H catalytic center of HIV-1 RT. As a consequence, Fe^{2+}-mediated hydroxyl radicals can be generated, which cleave *duplex DNA* at position −17 through an oxidative scission process. Although not demonstrated directly, this approach assumes that metal coordination occurs through the highly conserved acidic residues of the RNase H domain, namely Asp^{443}, Glu^{478}, Asp^{498}, and Asp^{549}. Since the DNase I footprinting data of Fig. 3 and RNase H activity of Fig. 4 suggest a greater separation of the RNase H and DNA polymerase catalytic centers of the Ty enzyme, we investigated whether this induced an altered patter of hydroxyl radical cleavage by Fe^{2+}-substituted Ty3 RT. The 71-nt DNA template/36-nt DNA primer depicted in Fig. 1 was employed for these studies. As predicted from studies with HIV-1 RT (32), cleavage of the template at position −17 is diagnosed by release of a 54-nt fragment (Fig. 5*A*).

Hydroxyl radical cleavage by Fe^{2+}-seeded p66/p51 HIV-1 RT, FIV RT, and the Ty3 enzyme was evaluated in parallel. As can be seen from the data of Fig. 5*B*, we were successful with both retroviral enzymes in Fe^{2+} substitution and hydroxyl radical cleavage at template nucleotide −17. In contrast, however, we failed to detect hydroxyl radical cleavage in the presence of Ty3 RT. The trivial possibility that Ty3 RT had lost activity during storage was eliminated in a parallel experiment in which RNase H activity was evaluated on an RNA/DNA hybrid in the presence of Mg^{2+}. Under these conditions, full activity for each enzyme was achieved (data not shown). In light of this, we hypothesized that residues important for Mg^{2+} coordination in HIV-1 and *E. coli* RT are less strictly conserved or are positioned differently in the Ty3 enzyme, thus affecting coordination geometry. The amino acid alignment presented in Fig. 7 indicates the counterparts of Asp^{443}, Glu^{478}, Asp^{498}, and Asp^{549} in the HIV-1 enzyme are preserved, so the absence of these conserved carboxylates can be ruled out. However, according to the revised model of Kashiwagi *et al.* (43), Asn^{474} and Gly^{444} of HIV-1 RT also participate in Mg^{2+} coordination at the RNase H domain, the counterparts of which are absent in the Ty3 enzyme. In addition, the monomeric nature of Ty3 RT may also influence the avidity with which Fe^{2+} is retained. Although these explanations are presently speculative, they indicate another significant difference between the retroviral and retrotransposon enzymes.

Initiation of Ty3 (+) Strand Synthesis—To determine whether the recombinant enzyme catalyzed more specialized activities required for accurate fulfillment of reverse transcription, we evaluated the capacity of Ty3 RNase H to excise the PPT primer from an RNA/DNA hybrid for extension into, and subsequent removal from, (+) strand DNA. Previous data from our laboratory (31, 44) have indicated that related retroviral enzymes will support each of these events in a single reaction. Our PPT "scanning" strategy is depicted in Fig. 6*A*, and investigates the recognition of both PPT- and non-PPT-containing RNA primers by the Ty3 enzyme. Primer P3 is complementary to (−) strand DNA sequences immediately 5′ to the sequence proposed to prime Ty3 (+) strand synthesis (20, 21). P3 thus evaluates the efficiency of non-PPT RNA-primed synthesis. P2 contains additional sequences 5′ to the PPT, and terminates within sites predicted to be most frequently used. Finally, P1 contains the Ty3 PPT and additional 3′ sequences, and must therefore be processed by Ty3 RNase H to reveal the authentic (+) strand primer. All experiments were performed in the presence of a dNTP mixture to reveal the steps of primer selection and extension. As an additional control, these primers

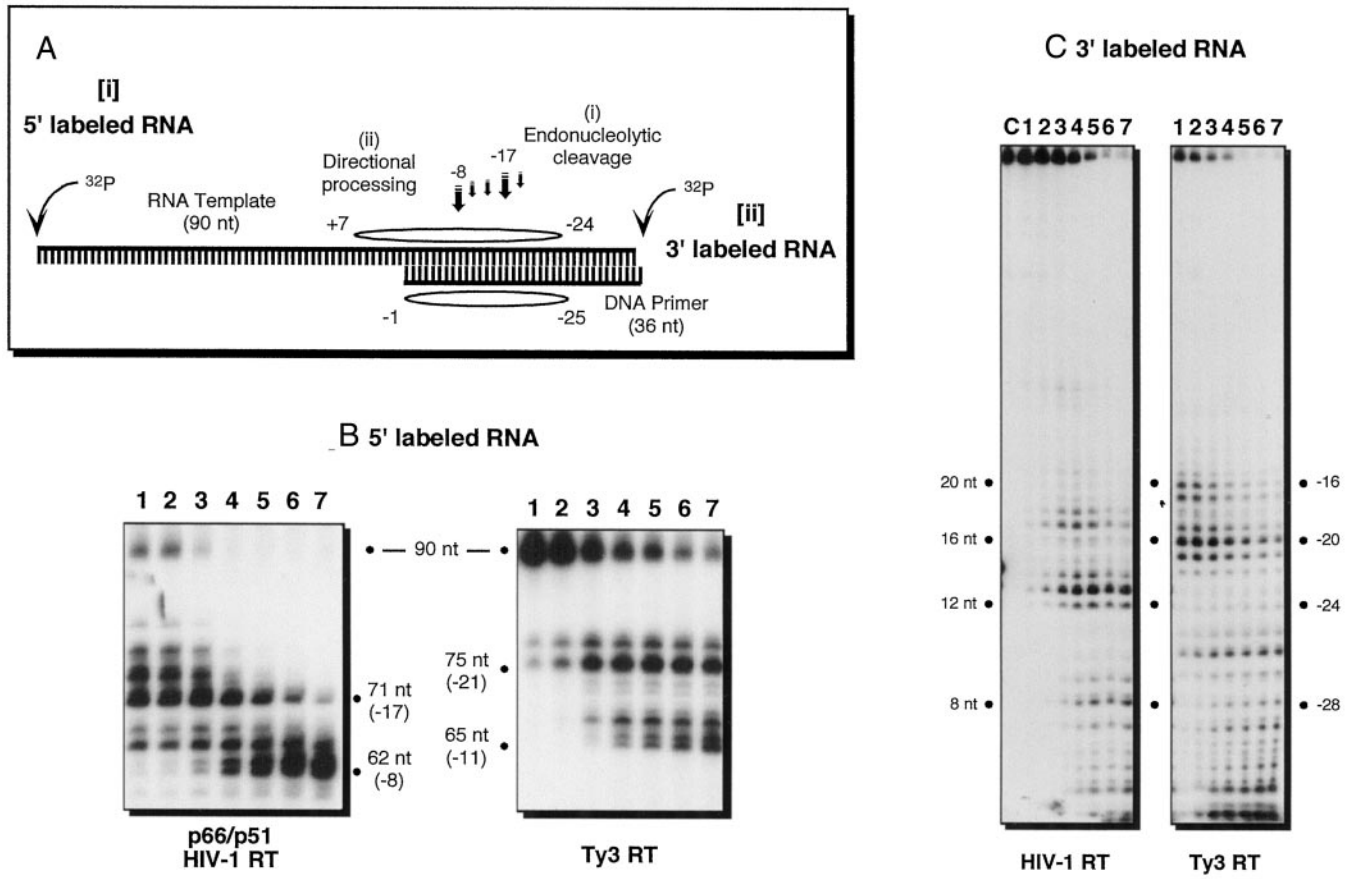

FIG. 4. **RNase H activity of purified Ty3 RT.** *A*, schematic representation of the substrates used for analysis. The major HIV-1-derived cleavage sites on the 90-nt RNA template have been indicated, designating the first base pair of the RNA-DNA hybrid in the DNA polymerase catalytic center "−1." *B*, HIV-1 and Ty3 hydrolysis profiles derived from substrate whose RNA 5′ terminus is ^{32}P-labeled. For both enzymes, hydrolysis was evaluated after 30 s (*lanes 1*), 1 min (*lanes 2*), 2 min (*lanes 3*), 5 min (*lanes 4*), 10 min (*lanes 5*), 20 min (*lanes 6*), and 40 min (*lanes 7*). The major sites of hydrolysis and corresponding fragment sizes are indicated at the *side* of each panel. *C*, hydrolysis profiles generated from substrate whose RNA 3′ terminus is ^{32}P-labeled. Time points *1–7* are similar to those in *B*, while *C* represents the uncleaved RNA template.

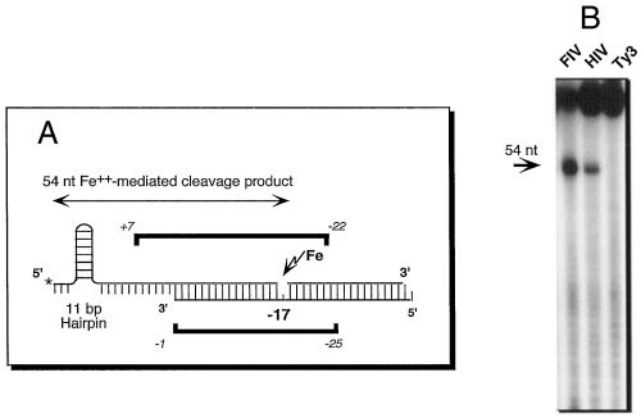

FIG. 5. **Ty3 RT fails to support Fe^{2+}-mediated cleavage of duplex DNA.** *Panel A* provides a schematic representation of the methodology. Substrate is the 71-nt template/36-nt primer used to evaluate DNA-dependent DNA polymerase. Template and primer nucleotides contacted by RT are indicated by the bars. Replacement of Mg^{2+} within the RNase H catalytic center with Fe^{2+} permits localized release of hydroxyl radicals and chemical scission at template nucleotide −17. When the template is radiolabeled at its 5′ terminus, Fe^{2+}-mediated hydroxyl radical cleavage generates a 54-nt hydrolysis product. *Panel B*, reactivity of HIV, FIV, and Ty3 RTs. The *arrow* indicates the position of the 54-nt cleavage product.

were extended by DNA polymerase I Klenow fragment, which efficiently recognizes their 3′ OH. The results of our investigation are presented in Fig. 6*B*.

While P1 and P2 were recognized by Ty3 RT, the data of Fig. 6*B* clearly indicate that the non-PPT RNA primer P3 does not support efficient (+) strand DNA synthesis, which is in keeping with reports on related systems (45–47). At this stage, we cannot determine whether this represents reduced affinity for the RNA-DNA hybrid or an inability of bound enzyme to catalyze DNA synthesis. (+) strand products of 40 and 27/26 nt accumulate when P1 is used as primer, the former of which is eliminated and the latter of which remains unchanged following NaOH treatment (to remove all ribonucleotides). Thus, the 40-nt species represents a (+) RNA/(+) DNA chimera, while the latter reflects RNase H-mediated primer removal following (+) strand DNA synthesis. That the "mature" DNA is a mixture of 27-nt and 26-nt species, rather than the predicted 25-nt species, indicates (*a*) that (+) strand synthesis initiation is slightly heterogeneous, and (*b*) the 3′ residue of primer P2 does not belong to the PPT.

(+) strand products of 50, 40, and 26/27 nt accumulate when P2 is used as primer. The largest corresponds to the intact primer (25 nt) covalently attached to (+) strand DNA, while the 40-nt product represents (+) strand DNA containing exclusively the PPT RNA primer. The shortest and principal products are 26/27 nt, resembling the "mature" DNA previously observed upon removal of primer derived from P1. In this case, however, these are shortened by a single nucleotide to 25/26 nt following alkaline hydrolysis. Hence, while initiation of (+) strand synthesis by Ty3 RT occurs without 3′ processing of primer P2, the resulting chimera is not cleaved by the enzyme at the RNA-DNA junction as observed in experiments using primer P1, but rather at an inter-ribonucleotide bond. This

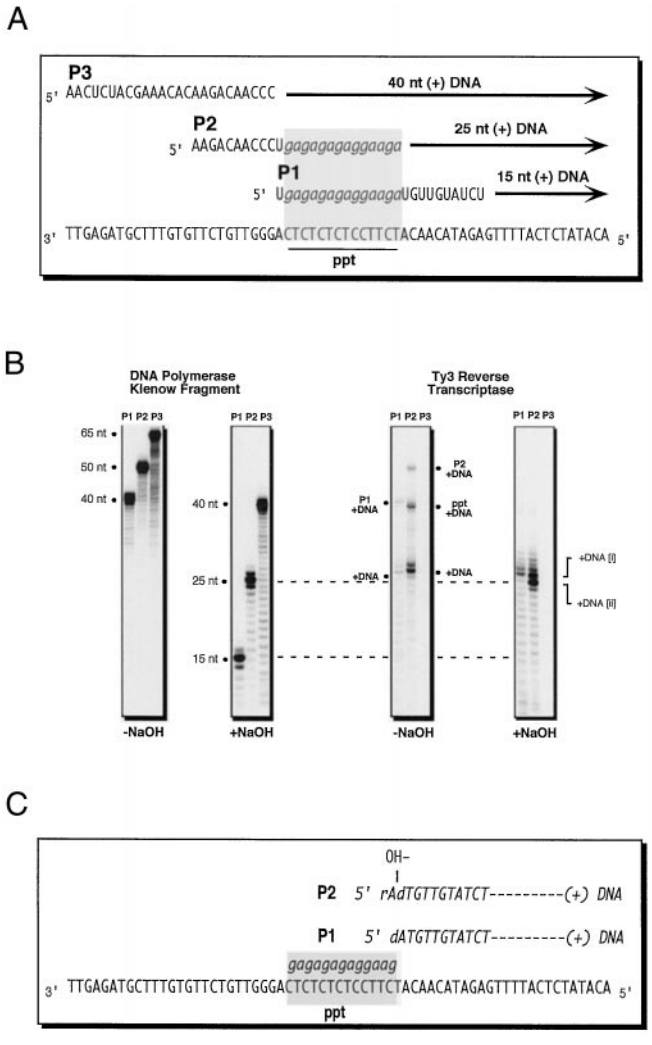

FIG. 6. **Selection and utilization of the Ty3 polypurine tract by purified Ty3 RT.** *A*, schematic representation of the model PPT selection/extension system. RNA oligonucleotides, 25 nt in length and designated P1, P2, and P3, were hybridized to a 65-nt DNA oligonucleotide. Within P1 and P2, *italicized*, lowercase ribonucleotides represent those of the PPT. P3 lies outside the PPT and thus serves as a control for RNase H and (+) strand initiation specificity. *B*, results of PPT selection/extension experiments. *Left panels* represent DNA synthesis profiles obtained with the Klenow fragment of DNA polymerase I, which efficiently recognizes RNA primers. *Right panels* represent the equivalent reactions catalyzed by Ty3 RT. In both *panels* denoted *+NaOH*, the RNA component of each DNA-RNA chimera was removed. *C*, summary of PPT selection and extension data with primers P1 and P2. Note that, while both (+) strand products generated by RT-associated RNase H activity are the same length, the 5′ terminal base is a ribonucleotide when P2 is used as primer. This ribonucleotide is subsequently removed following alkaline treatment. The PPT sequence most frequently used is located within the *shaded area*.

suggests that the recognition signal for primer removal is not the RNA-DNA junction, but an intrinsic feature of the polypurine tract structure.

DISCUSSION

Despite many similarities between retroviruses and LTR-containing retrotransposons, several recent reports underscore a need for an in-depth study of retrotransposon RTs and accessory proteins with which they might interact. First, documentation of a bipartite PBS in Ty3 (18) suggests that sequences at both ends of the (+) strand Ty3 RNA genome constitute the PBS and contribute to efficient initiation of (−) strand synthesis. This situation effectively places a discontinuous A-form duplex in the nucleic acid binding site, which is unlike any retroviral system. Second, Kirchner and Sandmeyer (21) and Wilhelm *et al.* (22) have found additional bases at the 3′ ends of the Ty3 upstream LTR, implying that RNase H-mediated selection and release of the PPT primer is less precise than demonstrated for retroviruses. Finally, Nymark-McMahon and Sandmeyer (48) have noted that mutations in the integrase (IN) component of he Ty3 *POL3* open reading frame have severe consequences for reverse transcription, implying an interaction between RT and IN, either as individual proteins or as the RT-IN polyprotein. In order to study reverse transcription in LTR-containing retrotransposons at the biochemical level, we have purified a 55-kDa protein representing the RT open reading frame of Ty3 and evaluated its interaction with nucleic acid duplexes encountered during replication, extending a recent *in vitro* evaluation of NC-mediated initiation of Ty3 reverse transcription (49) from the bipartite PBS.

The finding that purified enzyme migrated as a monomer by size exclusion chromatography, although surprising, is not unprecedented, since the same has been demonstrated for RT purified from bovine leukemia virus (33), MLV (36), and an active HIV-1/MLV chimera (50). In the case of MLV RT, it has been proposed that substrate binding induces dimerization, a feature we have not determined here. This was not the case for the bovine leukemia virus enzyme, which migrated to almost the same position in glycerol gradients in the absence and presence of substrate. Interestingly, the degree of similarity between the Ty3-*gypsy* family and certain retroviruses, in particular MLV, is sufficiently high that they have been speculated to comprise one large superfamily (16).

An unusual feature of our DNase I footprinting experiments is the 3–4-bp region of duplex DNA remaining accessible, and in some cases rendered hypersensitive, to nuclease digestion (Fig. 2, *C* and *D*). This region is substantially removed from the "window" of hydroxyl radical accessibility between positions −7 and −11 noted for the HIV-1 enzyme (41). This could reflect either an altered DNA structure or that the retrotransposon enzyme has independent nucleic acid binding domains separated by a flexible linker, as suggested for the MLV RT (36). Such spatial separation of functional domains may leave the intervening nucleic acid susceptible to nucleolytic cleavage. Furthermore, although the increased size of the footprint relative to HIV-1 and EIAV RT was unexpected, it is in keeping with the RNase H hydrolysis profiles of Fig. 4, supporting the notion that the spatial separation of the catalytic centers of Ty3 RT exceeds the 18 bp observed with most retroviral enzymes (37–39). Although speculative, it is worth noting in retroviruses that (*a*) the length of the tRNA:PBS duplex is 18 bp and (*b*) 18 bases of the tRNA primer are copied before (+) strand synthesis is interrupted and second strand transfer initiates (51). Thus, retroviral enzymes may have evolved to accommodate 18 bp of duplex between their catalytic centers to efficiently mediate two critical tRNA-mediated events in replication. In contrast, the equivalent events occur through entirely different mechanisms in Ty3. As indicated earlier, the Ty3 PBS is bipartite and is contributed from both ends of the genome. Moreover, nucleotides of $tRNA_i^{Met}$ constituting the PBS complement are not inherited by the element from the primer prior to second strand transfer in Ty1, as is the case in retroviruses (52). Although this has not been demonstrated for Ty3, it is possible that events normally requiring recognition or copying of 3′ nucleotides of the tRNA primer are more relaxed in retrotransposons and reflected in altered spatial coupling of the catalytic centers of their polymerases.

Data from both a heteropolymeric RNA/DNA hybrid (Fig. 4*B*) and substrates recapitulating selection, extension and release of the PPT primer (Fig. 5*B*) confirms a *bona fide* Ty3

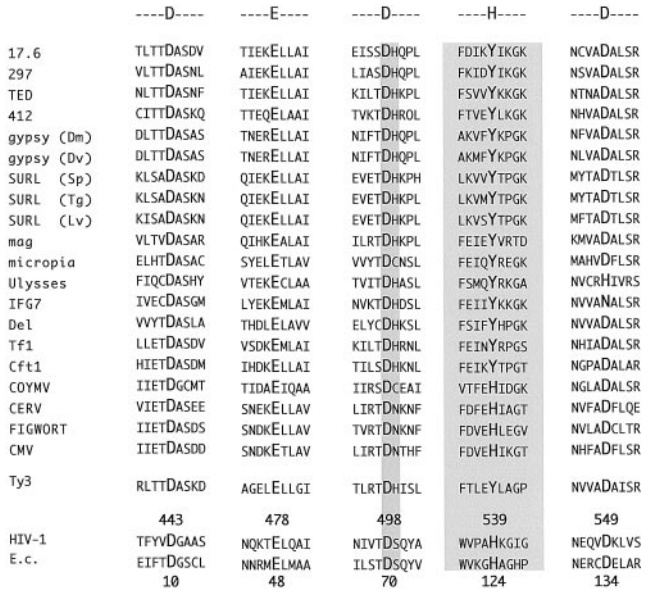

FIG. 7. **Alignment of catalytic residues in the RNase H domains of the *gypsy* group of retrotransposons and plant caulimoviruses.** The -D-D-D-H-E- preceding the compilation is derived from a comparison of the retroviral and bacterial enzymes, while *numbering above* and *below* HIV-1 RT and *E. coli* RNase H represents the amino acid positions. Within each *column*, the conserved residue is represented in *bold*. *17.6*, *297*, *412*, *gypsy*, *micropia*, and *Ulysses* are from *Drosophila*; *TED*, is from the cabbage looper; *SURL* elements are from echinoids; *mag* is from the silk moth *Bombyx mori*; IFG7 is from *Pinus radiata*; *Del* is from the lily, *Lilium henryi*; *Tf1* is from the fission yeast *Schizosaccharomyces pombe*; *Ty3* is from *S. cerevisiae*; *Cft1* is from *Cladosporium fulvum*. Plant caulimoviruses are abbreviated as follows: *COYMV*, Commelina yellow mottle virus; *CERV*, carnation etched ring virus; *FIGWORT*, figwort mosiac virus; *CMV*, cauliflower mosiac virus. The sequences presented have been modified from the phylogenetic relationships of Springer and Britten (55).

RNase H activity capable of performing highly specialized RNA processing events required during reverse transcription. An intriguing observation from the latter analysis is that the Ty3 enzyme initiates (+) strand synthesis from P1 and P2 with different specificity. Just as the recombinant enzyme was incapable of extending primer P3, extension of intact P1 was also inefficient, since the 3′ terminus is 10 nt removed from the PPT. Hence, the enzyme here must select its own initiation site via RNase H cleavage at the position indicated in Fig. 6*C*. Furthermore, since the smallest products generated from P1 are unchanged following sodium hydroxide treatment, the primer must be removed by RNase H-mediated cleavage at the RNA-DNA junction. This indicates that primer selection and removal occur at precisely the same site, *i.e.* within the -G-A-dinucleotide at the PPT 3′ terminus. In contrast, no RNase H processing seems to be required for initiation from primer P2. This would explain why it is utilized more efficiently than P1, which must be cleaved before DNA synthesis can occur. However, because the cleavage site for primer removal does not appear to vary between reactions, sites for initiation from and removal of P2-derived primers are separated by a single nucleotide. This is reflected in the difference between cleavage profiles for primer P2 following alkali treatment (Fig. 6*B*).

It is unclear why the primer selected by recombinant Ty3 RT differs by a single nucleotide from the principle site observed by Wilhelm *et al.* (21) *in vivo*. It is possible that sequences flanking the polypurine tract, and in part absent in primers P1 and P2, bias the cleavage specificity of the recombinant enzyme. Since multiple primers are selected in vivo, there is apparently some flexibility in the structural determinants for primer selection. Experiments designed to evaluate these determinants are currently under way.

Our data may also have implications for the general mechanism of RNase H-mediated hydrolysis, which has remained in doubt. Highly conserved residues of the HIV-1 RNase H domain include Asp^{443}, Glu^{478}, Asp^{498}, His^{539}, and Asp^{549}. According to Kashiwagi *et al*. (43), His^{539} serves as a general base (precedents for which are the enzymes DNase I and ExoIII), while Asp^{549} is involved in appropriately positioning a water molecule activated by His^{539} for electrophilic attack. This mechanism assumes participation of a single metal ion, which is clearly defined in the crystal structure of the bacterial enzyme (53, 54), and a role for the highly conserved His^{539}. The sequence compilation of Fig. 7 indicates good conservation of appropriately spaced acidic residues constituting the -D-E-D-D- motif within the RNase H domains of *gypsy* group of retrotransposons and plant caulimoviruses (55). However, two intriguing features in the former group, including Ty3 are: (*a*) substitution of this conserved histidine with an invariant tyrosine and (b) the emergence of a highly conserved histidine immediately adjacent to the counterpart of Asp^{498}. Conversely, plant caulimovirus RNases H and the retroviral and bacterial enzymes restore histidine at the equivalent of position 539, but now lack this residue immediately adjacent to Asp^{498}. One possibility we have considered from this compilation is that the cluster of catalytically conserved residues of *gypsy* group of retrotransposons is not -D-E-D-H-D-, but in fact -D-E-DH-D-, *i.e.* His of the adjacent Asp/His pair serves to activate a water molecule in the same manner that has been suggested for His^{539} and His^{124} of the HIV-1 and *E. coli* RNases H, respectively. The high degree of conservation of tyrosine in the "His box" suggests this serves a more structural role, possibly through a direct contact with the nucleic acid substrate. Current efforts are aimed at evaluating this proposal by *in vitro* site-directed mutagenesis, as well as to determine whether the His/Tyr pair in Ty3 RT can be interchanged.

Finally, although we can accurately recapitulate events mimicking initiation of (−) (49) and (+) strand synthesis (this work), interactions between RT and IN should not be overlooked, since several IN mutations result in reverse transcription defects in Ty3 virus-like particles (48). Such data imply an interaction between these polypeptides, either individually or as the RT/IN polyprotein. Efforts to prepare the 115-kDa Ty3 RT/IN polyprotein are presently under way.

Acknowledgments—We thank Kathryn J. Howard (Case Western Reserve University) for assistance in the preliminary purification of Ty3 RT, Suzanne B. Sandmeyer for critical reading of the manuscript, and John M. Coffin for insightful discussions.

REFERENCES

1. Leis, J., Aiyar, A., and Cobrinik, D. (1993) in *Reverse Transcriptase* (Skalka, A. M., and Goff, S. P., eds) pp. 33–47, Cold Spring Harbor Laboratory Press, Cold Spring Harbor, NY
2. Taylor, J. M., and Illmensee, R. (1975) *J. Virol.* **16,** 553–558
3. Cobrinik, D., Aiyar, A, Ge, Z., Katzman, M., Huang, H., and Leis, J. (1991) *J. Virol.* **65,** 3864–3872
4. Aiyar, A., Ge, Z., and Leis, J. (1994) *J. Virol.* **68,** 611–618
5. Miller, J. T., Ge, Z., Morris, S., Das, K., and Leis. J. (1997) *J. Virol.* **71,** 7648–7655
6. Wakefield, J. K., Wolf, A. G., and Morrow, C. D. (1995) *J. Virol.* **69,** 6021–6029
7. Li, Y., Zhang, Z., Kang, S.-M., Buescher, J. L., and Morrow, C. D. (1997) *Virology* **238,** 273–282
8. Zhang, Z., Kang, S.-M., Li, Y., and Morrow, C. D. (1998) *RNA* **4,** 394–406
9. Liang, C., Li, X., Rong, L., Inouye, P., Quan, Y., Kleiman, L., and Wainberg, M. S. (1997) *J. Virol.* **71,** 5750–5757
10. Isel, C., Ehresmann, C., Keith, G., Ehresmann, B., and Marquet, R. (1995) *J. Mol. Biol.* **247,** 236–250
11. Isel, C., Lanchy, J.-M., Le Grice, S. F. J., Ehresmann, C., Ehresmann, B., and Marquet, R. (1996) *EMBO J.* **15,** 917–924
12. Arts, E. J., Ghosh, M., Ehresmann, B., and Le Grice, S. F. J. (1996) *J. Biol. Chem.* **271,** 9054–9061
13. Arts, E. J., Stetor, S., Li, X., Rausch, J. W., Howard, K. J., Ehresmann, B., North, T. W., Goody, R. S., Wainberg, M. A., and Le Grice, S. F. J. (1996) *Proc. Natl. Acad. Sci. U. S. A.* **93,** 10063–10068
14. Lanchy, J. M., Keith, G., Le Grice, S. F. J., Ehresmann, B., Ehresmann, C., and

Marquet, R. (1998) *J. Biol. Chem.* **273,** 24425–24432
15. Isel, C., Westhof, E., Massire, C., Le Grice, S. F. J., Ehresmann, B., Ehresmann, C and Marquet, R. (1999) *EMBO J.* **18,** 1036–1046
16. Boeke, J., and Stoye, J. P. (1998) in *Retroviruses* (Coffin, J. M., Hughes, S. H., and Varmus, H. E., eds) pp. 343–432, Cold Spring Harbor Laboratory Press, Cold Spring Harbor, NY
17. Keeney, J. B., Champan, K. B., Lauermann, V., Voytas, D. F., Astrom, S. U., von Pawel-Rammingen, U., Byström, A., and Boeke, J. D. (1995) *Mol. Cell. Biol.* **15,** 217–226
18. Gabus, C., Ficheux, D., Rau, M., Kieth, G., Sandmeyer, S., and Darlix, J. L. (1998) *EMBO J.* **17,** 4873–4880
19. Friant, S., Heyman, T., Wilhelm, M. L., and Wilhelm, F. X. (1996) *Nucleic Acids Res.* **24,** 441–449
20. Brulé, F., Bec, G., Keith, G., Le Grice, S. F. J., Roques, B. P., Ehresmann, B., Ehresmann, C., and Marquet, R. (2000) *Nucleic Acids Res.* **28,** 634–640
21. Kirchner, J., and Sandmeyer, S. B. (1996) *J. Virol.* **70,** 4737–4747
22. Wilhelm, M., Heyman, T., Friant, S., and Wilhelm, F. X. (1997) *Nucleic Acids Res.* **25,** 2161–2166
23. Wohrl, B. M., Georgiadis, M., Telesnitsky, A., Hendrickson, W., and Le Grice, S. F. J. (1995) *Science* **267,** 96–99
24. Wohrl, B. M., Tantillo, C., Arnold, E., and Le Grice, S. F. J. (1995) *Biochemistry* **34,** 5343–5350
25. Rausch, J. R., Wohrl, B. M., and Le Grice, S. F. J. (1996) *J. Mol. Biol.* **257,** 500–511
26. Kirchner, J., and Sandmeyer, S. B. (1993) *J. Virol.* **67,** 19–28
27. Le Grice, S. F. J., and Grüninger-Leitch, F. (1990) *Eur. J. Biochem.* **178,** 307–314
28. Le Grice, S. F. J., Cameron, C. E., and Benkovic, S. J. (1995) in *DNA Replication: Methods in Enzymology* (Campbell, J. L., ed) pp 130–147, Academic Press, New York
29. Wohrl, B. M., Howard, K. J., Jacques, P. S., and Le Grice, S. F. J. (1994) *J. Biol. Chem.* **269,** 8541–8548
30. Ghosh, M., Cameron, C. E., Hughes, S. H., Benkovic, S. J., and Le Grice, S. F. J. (1995) *J. Biol. Chem.* **270,** 7068–7076
31. Rausch, J. W., and Le Grice, S. F. J. (1997) *J. Biol. Chem.* **272,** 8602–8610
32. Gotte, M., Maier, G., Gross, H. J., and Heumann, H. (1998) *J. Biol. Chem.* **273,** 10139–10146
33. Perach, M., and Hizi, A. (1999) *Virology* **259,** 176–189
34. Hansen, L. J., Chalker, D. L., Orlinsky, K. J., and Sandmeyer, S. B. (1992) *J. Virol.* **66,** 1414–1424
35. Ghosh, M., Jacques, P. S., Rodgers, D., Ottmann, M., Darlix, J.-L., and Le Grice, S. F. J. (1996) *Biochemistry* **35,** 8553–8562
36. Telesnitsky, A., and Goff, S. P. (1993) *Proc. Natl. Acad. Sci. U. S. A.* **90,** 1276–1280
37. Kohlstaedt, L. A., Wang, J., Friedman, M., Rice, P. A., and Steitz, T. A. (1992) *Science* **256,** 1783–1790
38. Jacobo-Molina, A., Ding, J., Nanni, R. G., Clark, A. D., Lu, X., Tantillo, C., Williams, R. L., Kamer, G., Ferris, A. L., Clark, P., Hizi, A., Hughes, S. H., and Arnold, E. A. (1993) *Proc. Natl. Acad. Sci. U. S. A.* **90,** 6320–6324
39. Huang, H., Chopra, R., Verdine, G. L., and Harrison, S. C. (1998) *Science* **282,** 1669–1675
40. Arts, E. J., and Le Grice, S. F. J. (1998) *Prog. Nucleic Acid Res. Mol. Biol.* **58,** 339–393
41. Metzger, W., Hermann, T., Schatz, O., Le Grice, S. F. J., and Heumann, H. (1993) *Proc. Natl. Acad. Sci. U. S. A.* **90,** 5909–5913
42. Gotte, M., Maier, G., Onori, A. M., Cellai, L., Wainberg, M. A., and Heumann, H. (1999) *J. Biol. Chem.* **274,** 11159–11169
43. Kashiwagi, T., Jeanteur, D., Haruki, M., Katayanagi, K., Kanaya, S., and Morikawa, K. (1996) *Protein Eng.* **9,** 857–867
44. Stetor, S. R., Rausch, J. W., Boone, L. R., and Le Grice, S. F. J. (1999) *Biochemistry* **23,** 3656–3667
45. Randolph, C. A., and Champoux, J. J. (1994) *J. Biol. Chem.* **269,** 19207–19215
46. Fuentes, G. M., Rodriguez-Rodriguez, L., Fay, P. J., and Bambara, R. A. (1995) *J. Biol. Chem.* **270,** 28169–28176
47. Powell, M. D., and Levin, J. G. (1996) *J. Virol.* **70,** 5288–5296
48. Nymark-McMahon, M. H., and Sandmeyer, S. B. (1999) *J. Virol.* **73,** 453–465
49. Cristofari, G., Gabus, C., Ficheux, D., Bona, M., Le Grice, S. F. J., and Darlix, J. L. (1999) *J. Biol. Chem.* **274,** 36643–36648
50. Misra, H. S., Pandey, P. K., and Pandey, V. N. (1998) *J. Biol. Chem.* **273,** 9785–9789
51. Burnett, B. P., and McHenry, C. S. (1997) *Proc. Natl. Acad. Sci. U. S. A.* **94,** 7210–7215
52. Lauermann, V., and Boeke, J. D. (1997) *EMBO J.* **16,** 6603–6612
53. Katayanagi, K., Miyagawa, M., Matsushima, M., Ishikawa, M., Kanaya, S., Nakamura, H., Ikehara, M., Matsuzaki, T., and Morikawa, K. (1992) *J. Mol. Biol.* **223,** 1029–1052
54. Katayanagi, K., Ishikawa, M. Okumura, M., Ariyoshi, M., Kanaya, S. Kawano, Y., Suzuki, M., Tanaka, I., and Morikawa, K. (1993) *J. Biol. Chem.* **268,** 22092–22099
55. Springer, M. S., and Britten, R. J. (1993) *Mol. Biol. Evol.* **10,** 1370–1379